Supplementary Figures and Legends:

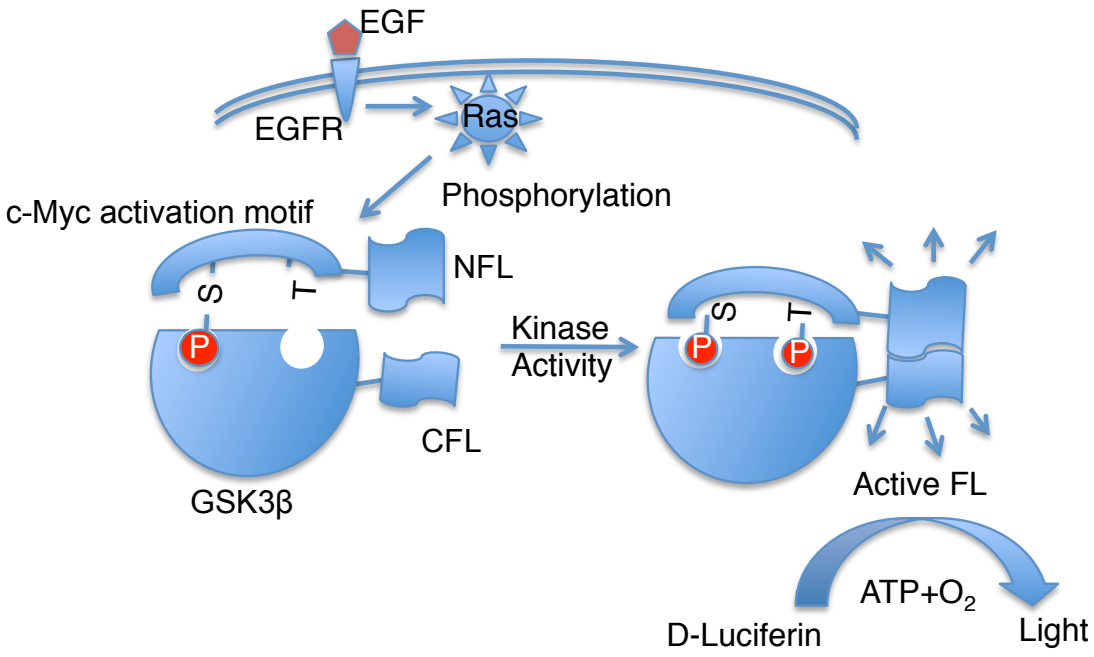

Fig. S1. Scheme of the c-Myc activation sensor. Upon growth factor stimulation, such as EGF binding to its receptor EGFR, Ras is activated and induces phosphorylation of c-Myc activation motif at Ser-62 (S62). Phosphorylated S62 is recognized by GSK3β, which further phosphorylates Thr-58 (T58) through its intrinsic kinase activity. This interaction brings two split Firefly luciferase fragment NFL and CFL, which are fused with the c-Myc activation motif and GSK3β binding domain respectively, into close proximity and induces complementation and reconstitution of Firefly luciferase (FL) activity, which produces light upon addition of its substrate D-Luciferin.

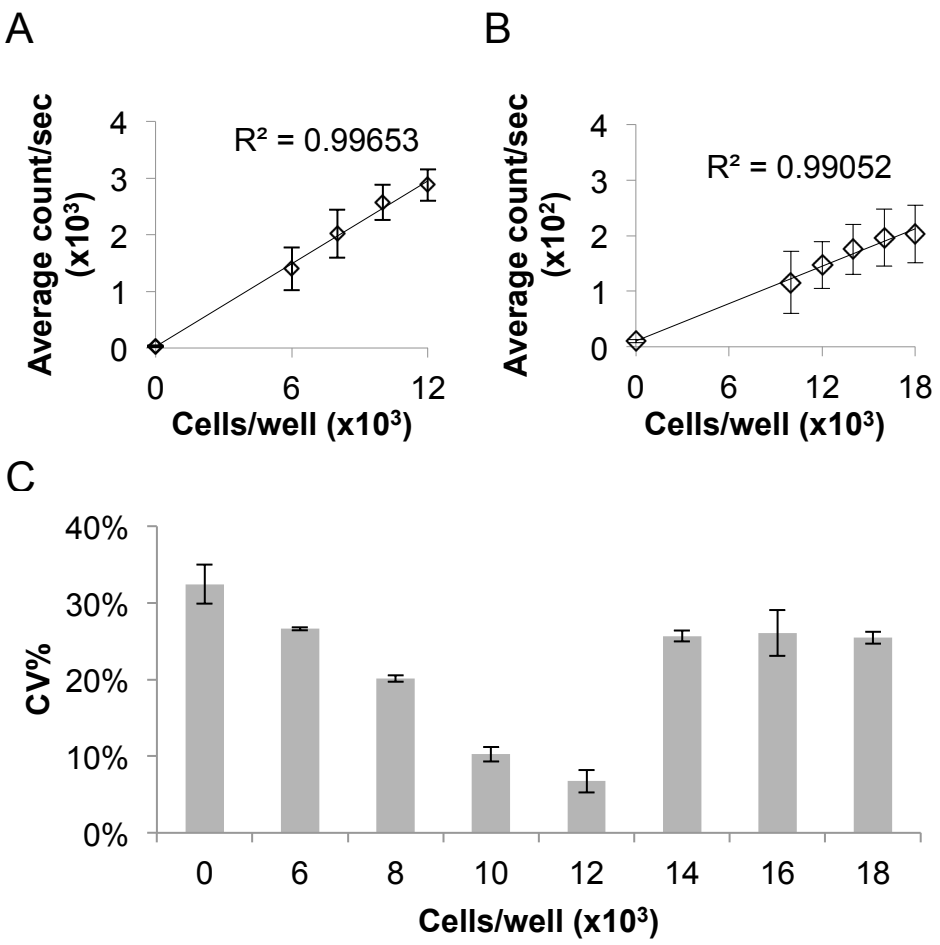

Fig. S2. Optimal cell plating numbers for HTS format. SK-ST cells were plated in 384 well plates with increasing cell numbers from 6,000 to 18,000 cells per 100µl each well (A and B) and imaged for the FL activity. Percentage of Coefficient of variation (CV) was measured for each cell concentration (C).

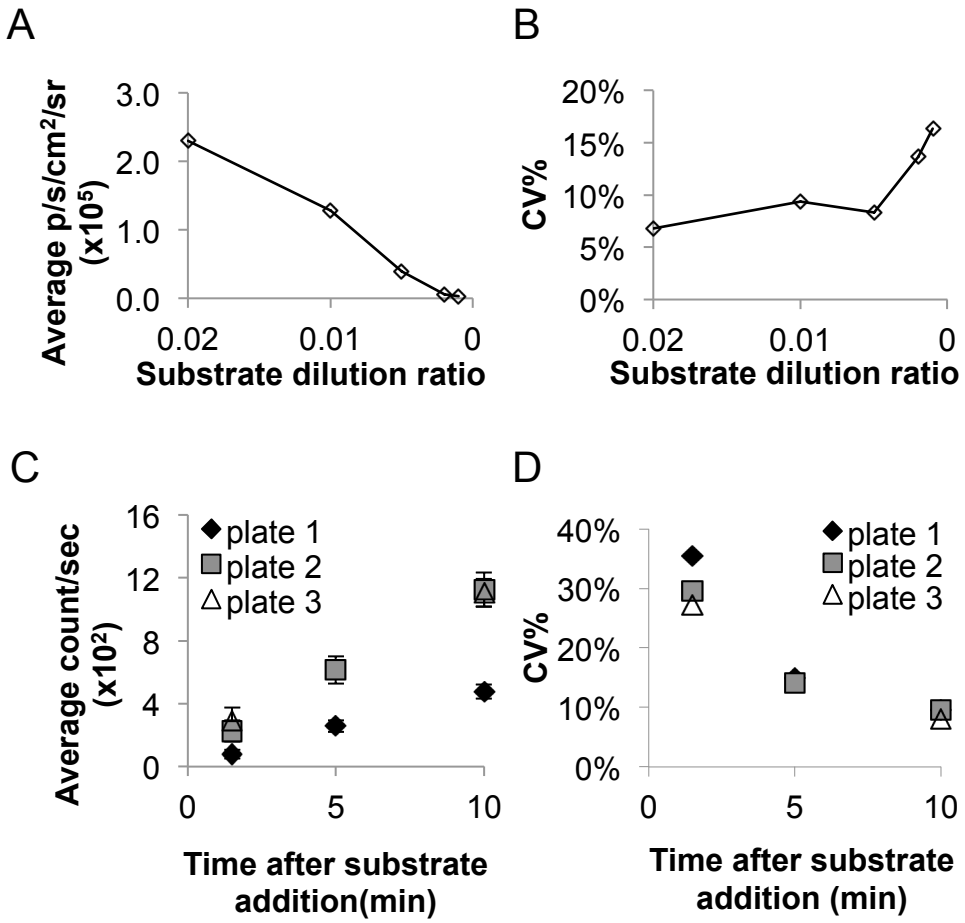

Fig. S3. Optimal substrate concentration and imaging time for HTS format. 45mg/ml stock D-Luciferin substrate was added with 50, 100, 200, 500 and 1000 fold dilution, each into 2 columns of a 96 well plate. Cells were imaged 2mins after substrate addition in IVIS 50 (A). Percentage of CV for each dilution was calculated (B). Stock D-Luc was added in 50 fold dilution into three 384well plates with 12,000 cells per well. Signals of each plate were counted at 2, 5 and 10mins after substrate addition and the percentage of CV of each plate at each time point was calculated (C).

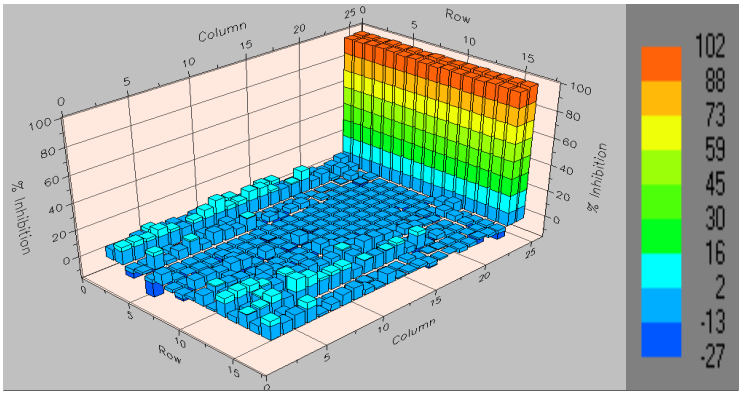

Plate#	Ave	Stdv	CV%	Z factor
1	1203.76	137.07	11.4%	0.66
2	1240.44	122.59	9.9%	0.70
3	1285.09	126.02	9.8%	0.71
4	1299.85	121.19	9.3%	0.72
5	1333.06	131.46	9.9%	0.70
6	1259.65	136.48	10.8%	0.67

Fig. S4. Robustness of the cell assay. 12,000 cells were plated in each well of the 1-22 columns of six 384 well plates for 24hrs. 23-24 columns of all the plates were added with cell medium only. 50 fold dilution of 45mg/ml stock D-Luc was added to each well and counted for FL signal 10mins after addition. A representative 3D graph of the signal of each well in 384 well plates was plotted as percentage of inhibition. The average signal intensity, its standard deviation, the CV and Z factor of each plate were calculated.

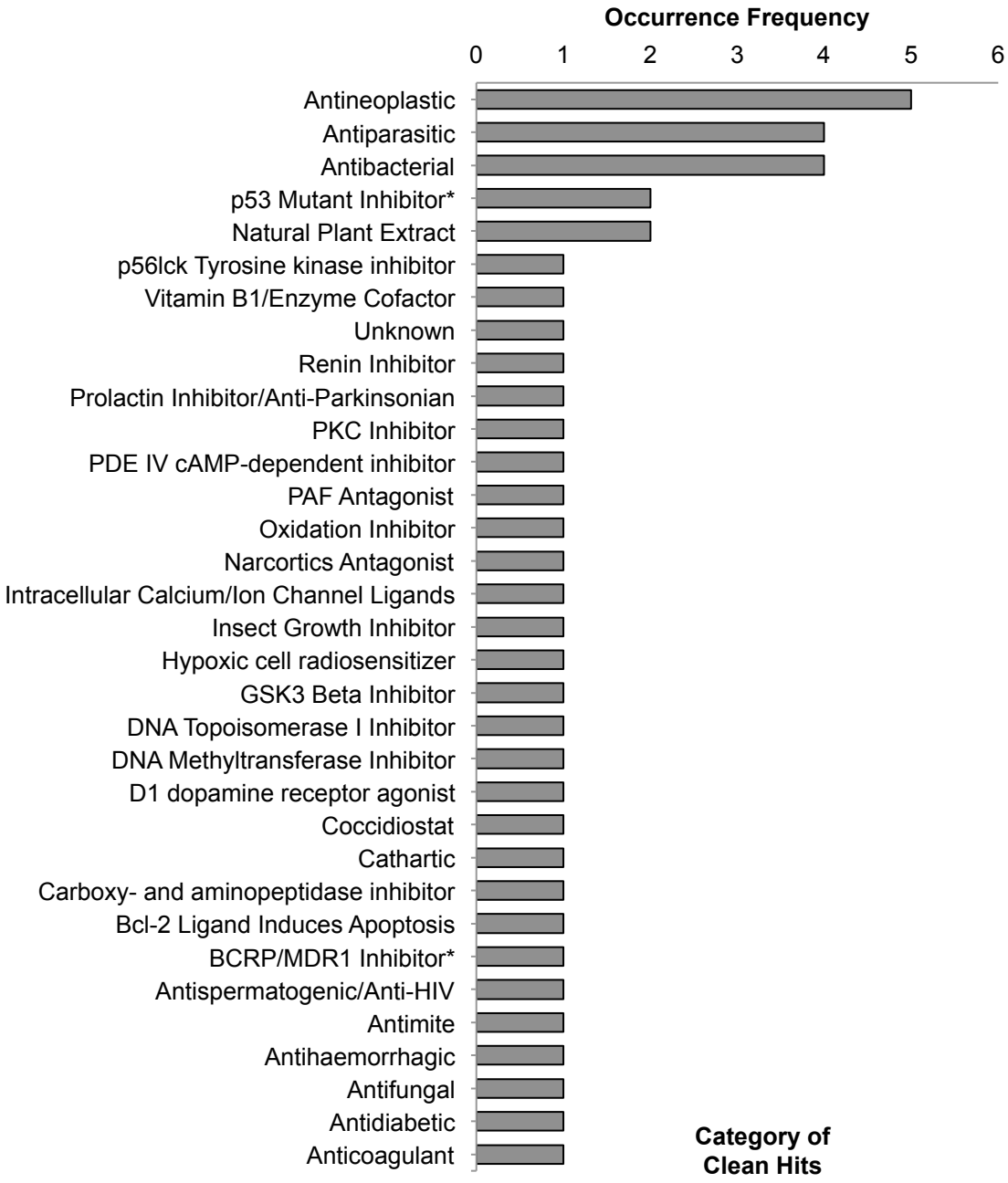

Fig. S5. Plot of the occurrence frequency of compound classes for all the clean hits from five libraries. * based on deposited HTS data in PubChem.

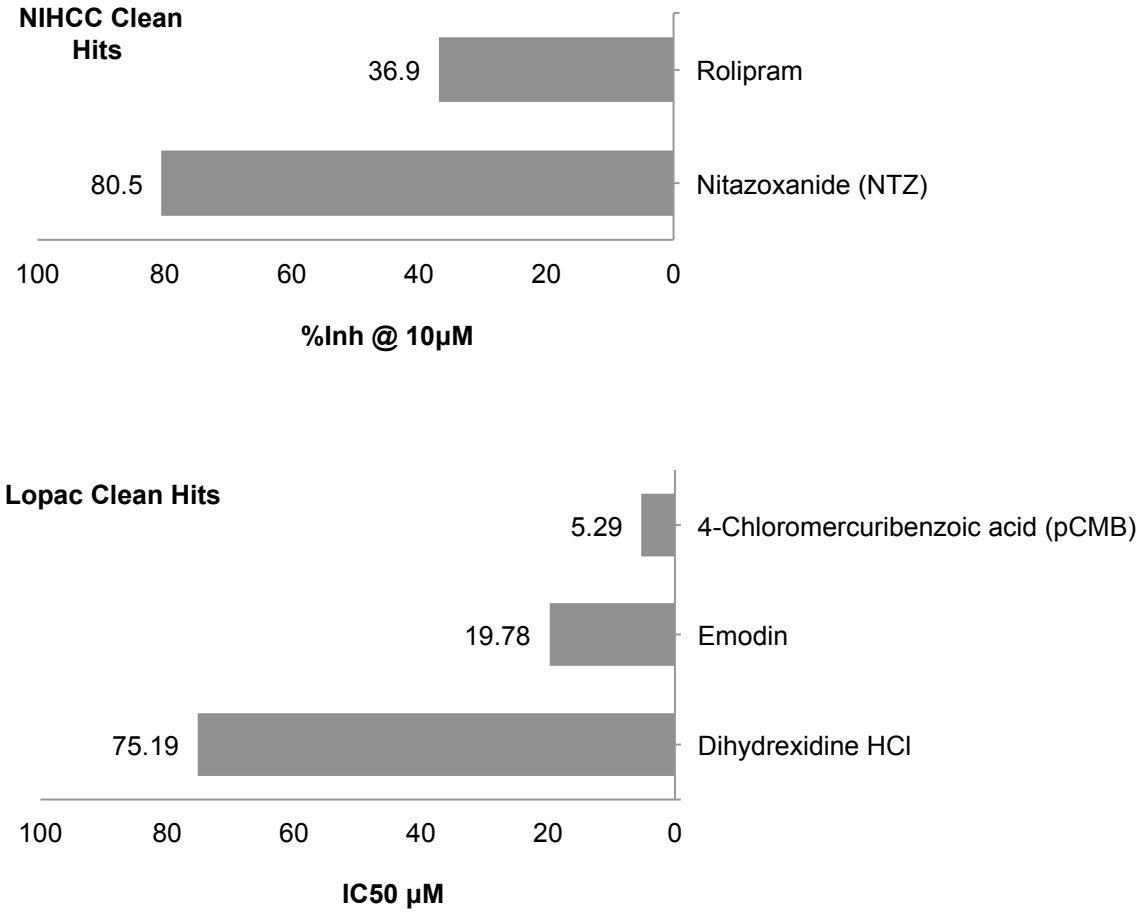

Fig. S6. The percent inhibition at 10µM of all the clean hits from the NCC library and the IC50 of all the clean hits from the Lopac library are plotted.

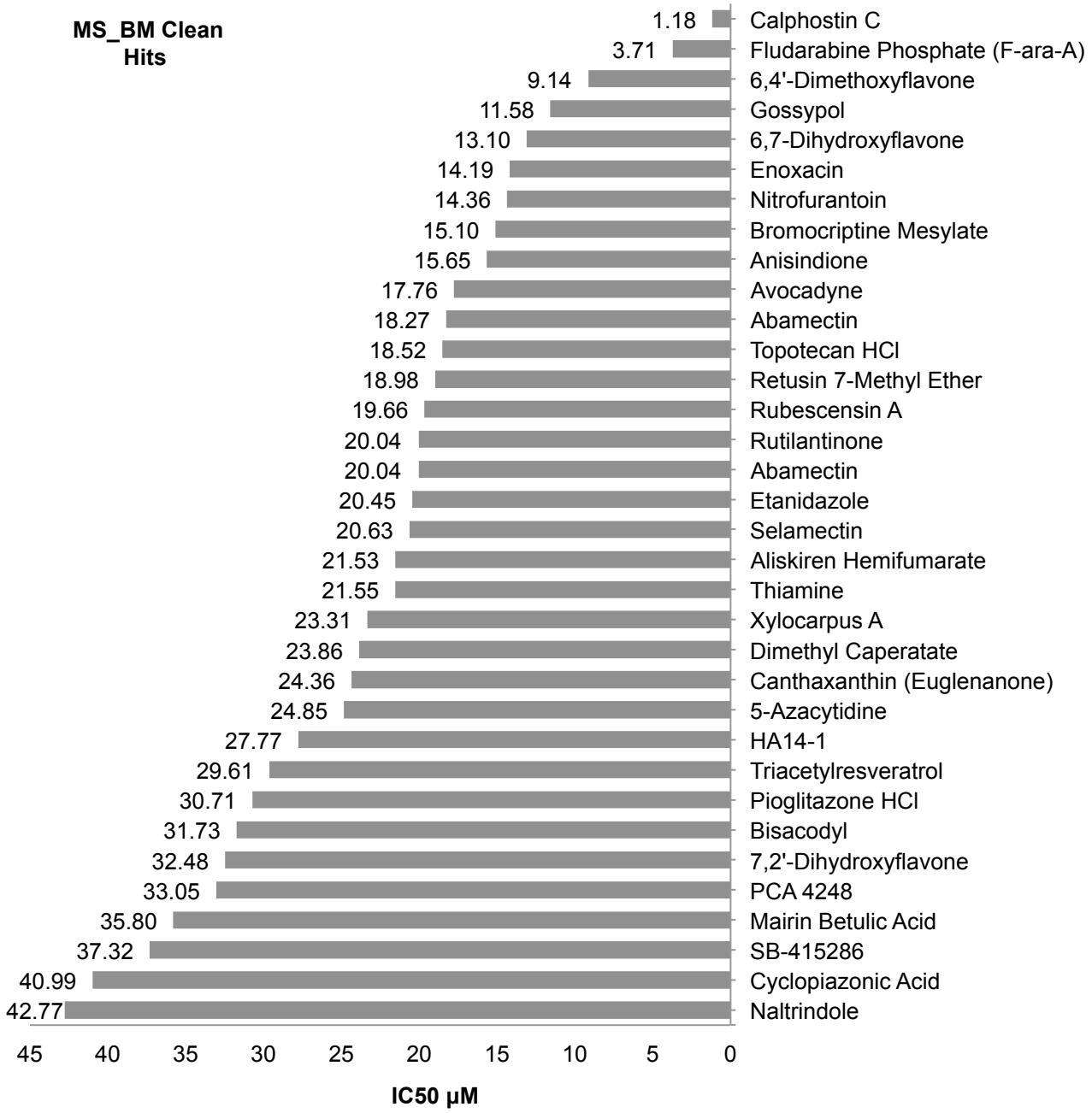

Fig. S7. Plot of IC50 of all the clean hits from combined MS, BMI and BMF libraries.

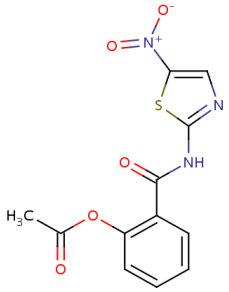

Nitazoxanide (NTZ)

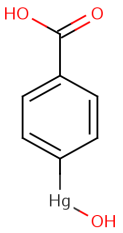

4-Chloro mercuribenzoic acid (pCMB)

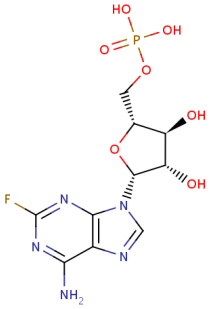

Fludarabine Phosphate (F-ara-AMP)

Compound	% inhibition at 10μM	IC50 (μM)
NTZ	80.5	ND
pCMB	85.3	5.29
F-ara-AMP	90.3	3.71

ND: not determined

Fig. S8. The top three unexpected potent hits. The chemical structures of the three most potent hits that were not previously described to have an inhibitory effect on c-Myc are shown. The percentage inhibition at 10μM and the IC50 for each drug are listed.

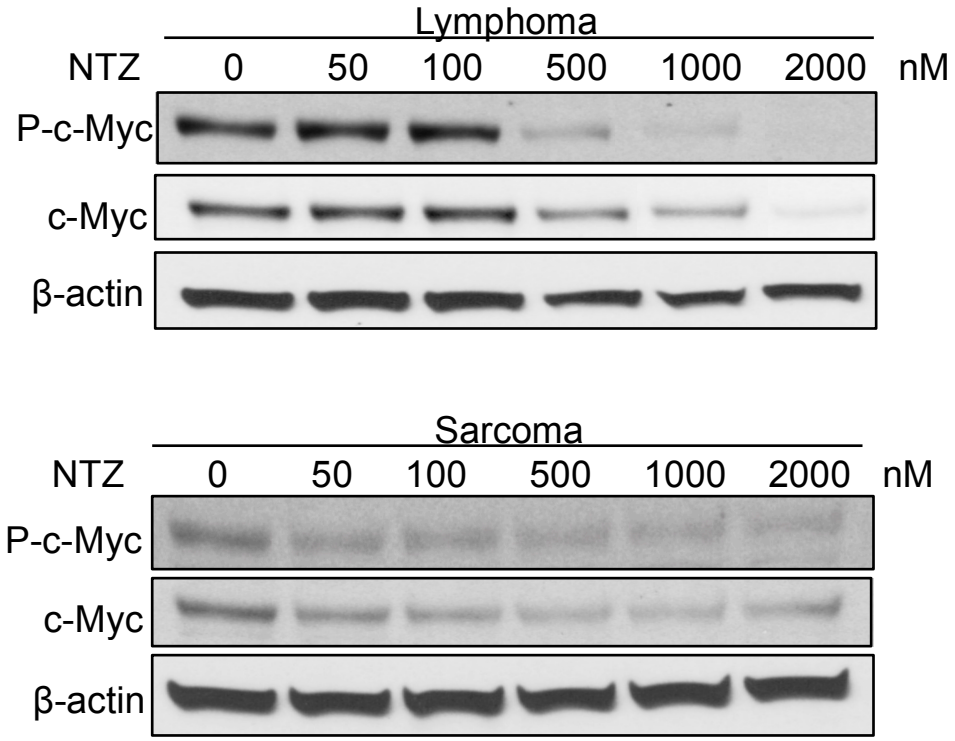

Fig. S9A. Western blot analysis of lymphoma and sarcoma cells after NTZ treatment was performed using phospho c-Myc, c-Myc protein and β-actin antibodies.

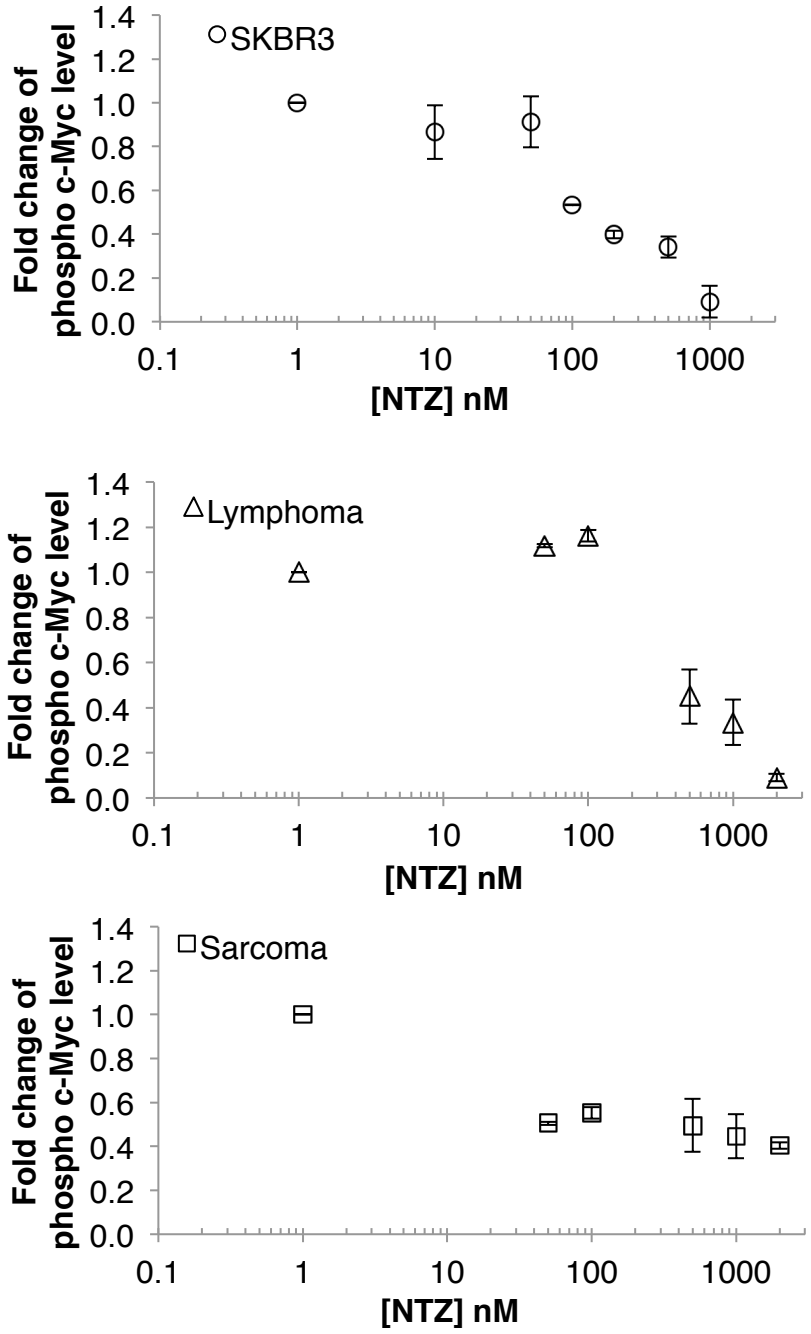

Fig. S9B. Dose dependent inhibition of phospho c-Myc by NTZ in different cancer cell lines. The fold-change of phospho c-Myc level was plotted against the log scale of NTZ concentration. Each point indicates the mean fold change of phospho c-Myc level of 2-3 different WB analyses and the error bar is the ±SD.

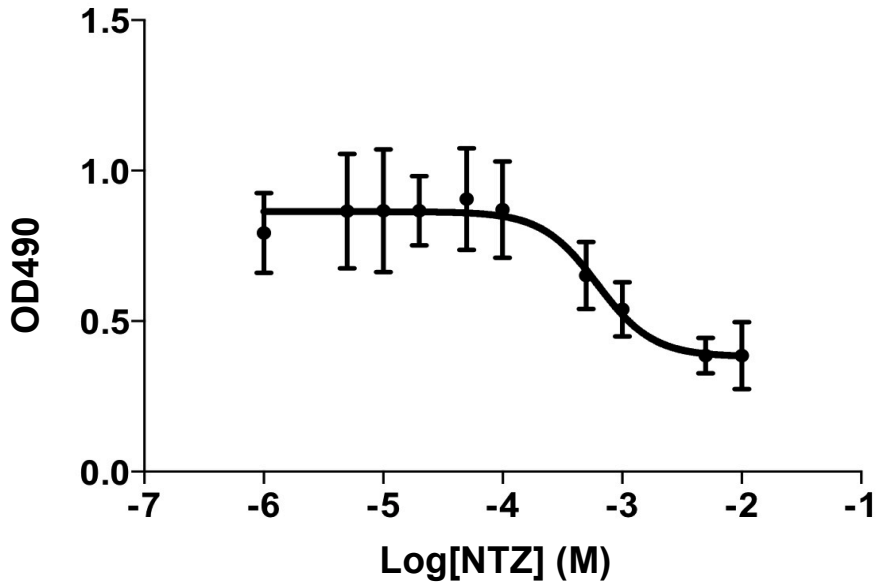

Fig. S10. Effect of NTZ on cell viability. $1x10^5$ SKBR3 cells were plated in each well of the 96 well plate for 24hrs. Indicated NTZ concentrations were each plated to one column of the plate. MTS assay was performed on each well. OD490 was plotted against log molar concentration of NTZ.

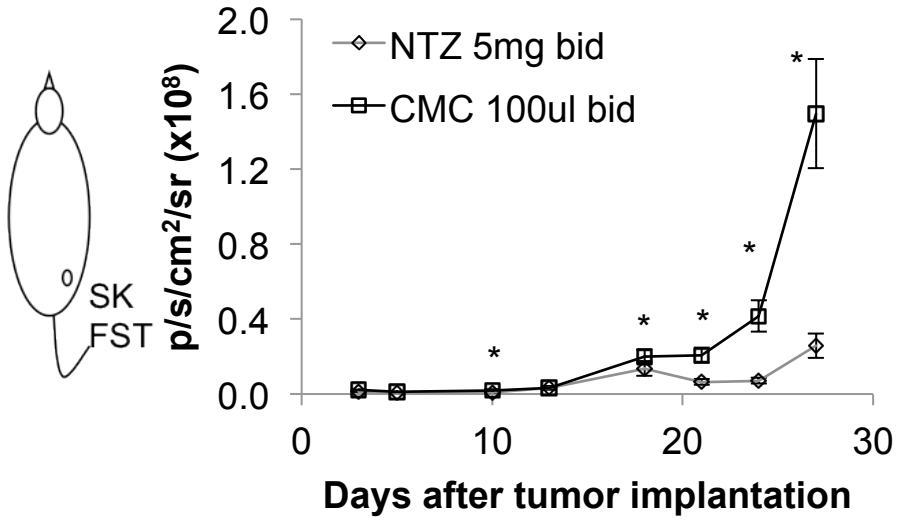

Fig. S11. In vivo efficacy of NTZ in a SK-FST xenograft model. SK-FST stable cells were s.c. implanted as indicated and treated with NTZ or CMC as described in Material and Methods. Photon output of SK-FST cells with NTZ or CMC treatment was plotted against days after implantation. * P<0.05.

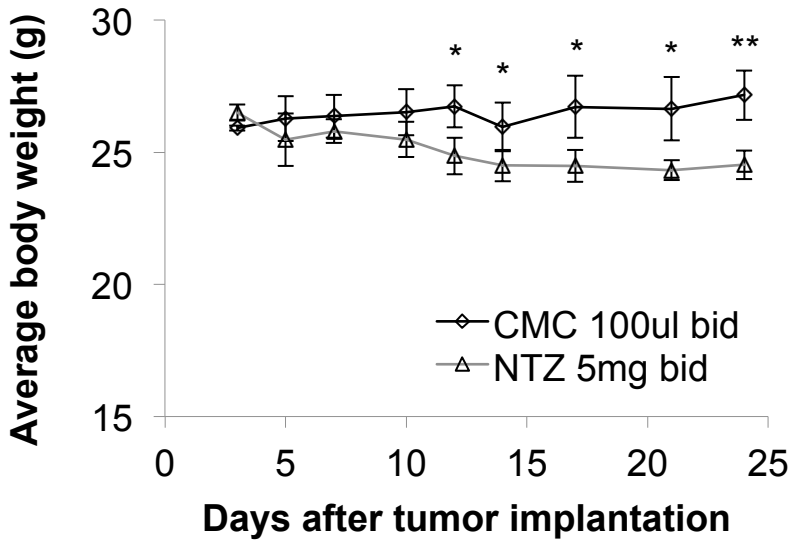

Fig. S12. Plot of the average body weight of NTZ or CMC treated group at indicated days after implantation. * P<0.05, ** P<0.01.

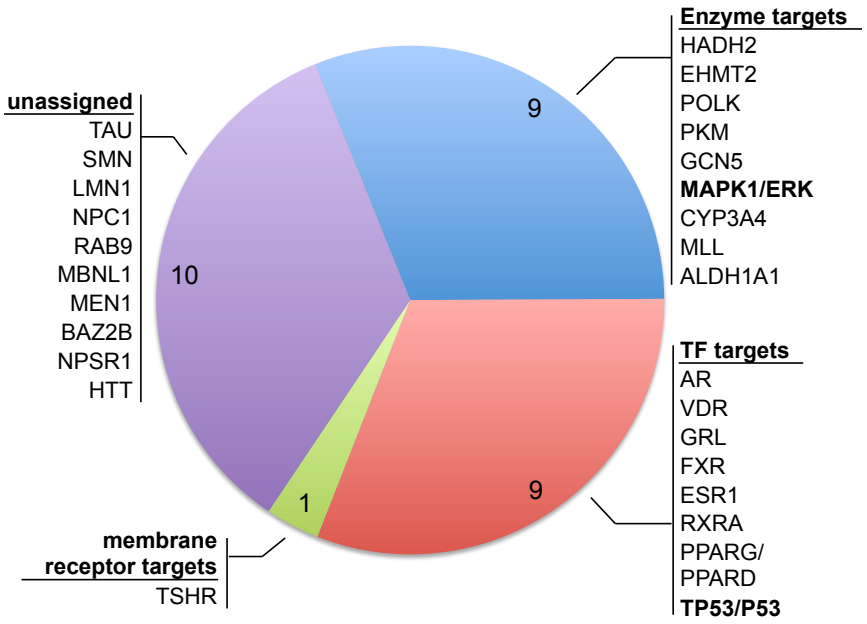

Fig. S13. Categories of NTZ targets in human based on CHEMBL database. Number of targets in each category is indicated. Highlighted are c-Myc related targets, MAPK1/ERK and TP53/P53.